A continuous monitoring approach for ecosystems based on time series analyses: A proposal with a case study for the mangroves of Marismas Nacionales, Mexico

Samuel Velázquez-Salazar [1], Inder Tecuapetla-Gómez[1,2], Cecilia Cervantes-Rodríguez [3]

[1] Geomatics Unit, National Commission for the Use and Knowledge of Biodiversity (CONABIO), Mexico City 14010, Mexico
[2] Investigadores por México, Secretary of Science, Humanities, Technology and Innovation, Mexico City 03940, Mexico - itecuapetla@conabio.gob.mx
[3] Department 'El Hombre y su Ambiente', Metropolitan Autonomous University, Xochimilco 04960, Mexico

Keywords: mangroves, Marismas Nacionales, time series, Sentinel-2, NDVI, Mann-Kendal test, trends.

Abstract

The mangrove ecosystem stands out for the numerous environmental services it provides, in addition to being one of the most vulnerable ecosystems to climate change. Marismas Nacionales is located in northwestern Mexico and hosts one of the most extensive areas of continuous mangrove ecosystem along the Pacific North coast of Mexico. Although vital, this mangrove ecosystem faces multiple pressures and is shifting inland in response to climate change —making ongoing monitoring of its size and health essential. Aiming for monitoring the health of mangrove and disturbed mangrove areas, a time series of monthly NDVI composites derived from Sentinel-2 imagery (10 m spatial resolution) was analyzed for the period 2019–2024. At the pixel level, the Mann-Kendall test was applied to determine significant trends. An inspection of the Z-statistic was conducted to identify gradual and relevant changes; when possible, these changes were validated with field data and high-resolution imagery. The results revealed heterogeneity in the behavior of pixel time series, reflected in the values of the Z-statistic. This heterogeneity is due to the fact that mangroves are subject to different change factors depending on their spatial location. Among the key factors identified were hurricane-induced damage, land-use change, inland colonization, recovery driven by restoration efforts, post-hurricane vegetation rebound, and losses resulting from coastal erosion. Across the 80,959 hectares encompassed by the study area, 47.08% exhibited a significant negative trend, 20.19% a non-significant negative trend, 18.07% a non-significant positive trend, and 14.66% a significant positive trend. The analyzed data revealed the dynamic nature of the mangrove ecosystem in response to various change factors, and the proposed method could serve as a foundation for integration into the national products generated by Mexico's Mangrove Monitoring System.

1. Introduction

Mangroves are dynamic ecosystems dominated by tree-like plant species known as mangles. They are typically found along the coastal zones of tropical and subtropical regions worldwide; in Mexico, they occur along both the Atlantic and Pacific coasts. These ecosystems are critically important due to the wide range of ecosystem services they provide—supporting, provisioning, regulating, and cultural—including flood control, greenhouse gas capture, nutrient supply to neighboring ecosystems such as coral reefs, habitat and protection for various species, and defense against hurricanes, (Velázquez-Salazar et al., 2021). Mangroves possess adaptations that allow them to thrive in challenging intertidal environments, enduring extreme conditions such as strong tidal currents, tropical storms, and hurricanes (Abu Bakar et al., 2024). Additionally, their root systems stabilize sediments and mitigate the impact of strong winds and wave action, (Ferreira et al., 2023).

Despite their resilience and numerous adaptations that allow them to withstand extreme climatic conditions, mangroves remain vulnerable to the adverse effects of natural atmospheric phenomena such as hurricanes, which are characterized by strong winds, torrential rains, and intense low-pressure systems (Floriano et al., 2025). Hurricanes are classified according to the Saffir-Simpson scale, ranging from Category 1 (119–153 km/h) to Category 5 (over 252 km/h) (Islam and Assal, 2023). These events can obstruct tidal channels, thereby disrupting the water exchange processes essential for nutrient flow and oxygenation in mangrove ecosystems. Additionally, hurricanes can break branches or damage the main trunks of mangrove trees (Hao et al., 2024).

In addition to facing the adverse effects of natural atmospheric phenomena, mangroves are under constant pressure from various human activities related to land-use change. The establishment of aquaculture farms, urban expansion, and road construction are just a few examples that threaten their ecological integrity and contribute to the growing list of change drivers. Assessing and monitoring these types of impacts is challenging due to factors such as the vast extent and limited accessibility of mangrove areas. Consequently, remote sensing techniques have become an essential tool for tracking the condition of mangroves. Through the use of satellite imagery, large-scale and high-resolution data can be collected on the state of mangroves during various change processes.

In this regard, the objective of the present study is to analyze a time series of NDVI derived from Sentinel-2 imagery as a foundation for the continuous monitoring of ecosystem stability conditions, specifically in mangrove environments. As a case study, we focus on the mangroves of Marismas Nacionales—a complex lagoon system that contains the most extensive mangrove coverage along Mexico's Pacific coast. Our approach to continuous monitoring relies on the application of computationally efficient and robust statistical tools, such as trend analysis based on the Mann-Kendall test, across the entire area of in-

terest. As a complement, trends in specific zones of particular interest —identified a priori as having undergone gradual or abrupt change— are classified according to characteristics of natural regeneration or potential active restoration.

2. Methodology

2.1 Study area

Marismas Nacionales, see Figure 1, is the largest mangrove-estuarine system on the eastern Pacific coast (170,000 ha) and is located at the coordinates N21°53′99″, S20°36′, E103°43′ and W105°46′, (de la Lanza Espino et al., 2010), (Vizcaya-Martínez et al., 2022). This wetland is formed by estuarines, coastal lagoons, tidal channels and rivers, which are home to a large number of endemic and migratory species of ecological and conservation importance, (Valderrama-Landeros et al., 2025).

2.2 Dataset

We have used monthly composites of the Normalized Difference Vegetation Index (NDVI) from the Harmonized Copernicus Sentinel-2 collection ("COPERNICUS/S2_SR_HARMONIZED"), available through the Google Earth Engine (GEE) platform. The period of study was January 2019 to December 2024. We recall that NDVI is defined as:

$$NDVI = (NIR - RED)/(NIR + RED),$$

where NIR and RED denote the infrared and red spectral bands, respectively. It is well-known that for Sentinel-2 scenes, the NIR and RED are located in the bands 8 and 4, respectively. The monthly composite that we utilized was generated with the following criteria: for any scene, at the pixel level, the maximum NDVI value was considered and subsequently, the arithmetic mean of the images within the month was calculated. As a quality filter we only considered scenes with less than 15% of cloudiness.

2.3 Area of interest

A mangrove mask was created using mangrove and disturbed mangrove coverage data from the years 2015 and 2020, generated by the National Commission for the Knowledge and Use of Biodiversity (CONABIO). Disturbed mangrove areas include wetlands with dead or regenerating mangrove stands, as well as mangrove forest cover altered by tropical storms, hurricanes, or anthropogenic infrastructure (e.g., hydraulic works, highways, and roads). These criteria are based on classification categories defined within the descriptive framework of Mexico's Mangrove Monitoring System (SMMM), developed by CONABIO, cf. (Valderrama et al., 2014).

These layers were intersected to produce a composite layer and delimit the area of interest (AOI) of this study. A 10-meter buffer was applied to the resulting layer to ensure a one-pixel margin of error. Subsequent processing was carried out using the R programming language (R Core Team, 2023). A mosaic was generated to merge the annual raster datasets, which had been separated into chunks by GEE. Additionally, a mask was applied to these annual mosaics based on the AOI.

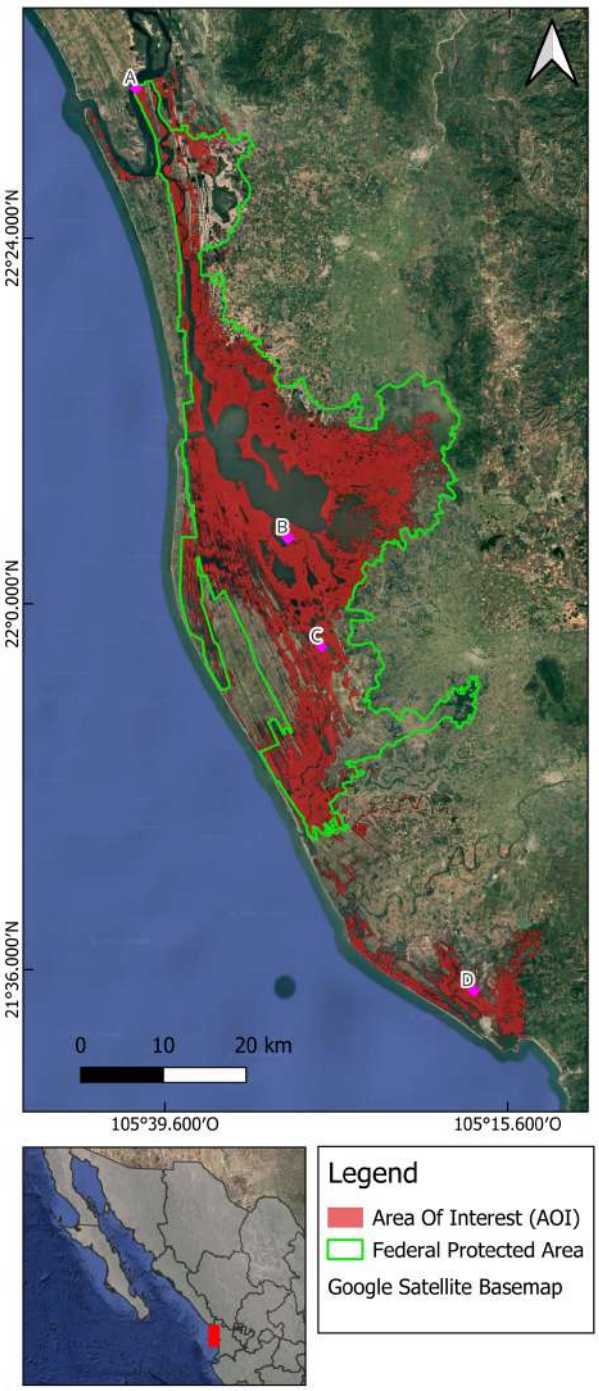

Figure 1. Study area and delimitation of the AOI.

2.4 TATSSI

The time series comprised of monthly NDVI composites from 2019 to 2024 was analyzed using the TATSSI platform (Tecuapetla-Gómez et al., 2021). Within this platform, two statistics were calculated to assess dataset quality: the percentage of missing data and the number of consecutive missing values (max-gap length) per time series at the pixel level. For time series with missing data, gaps were filled using ordinary linear interpolation. Finally, the Mann-Kendall test was applied to each time series to identify pixels exhibiting significant positive or negative trends; the significance level used was $\alpha = 0.05$.

2.5 Additional trend classification

In order to improve our understanding of some dynamics occurring at neighborhoods of points **B** and **C** in Figure 1, a further trend classification was conducted in two data *chips* located in these zones. These chips are subsets of the NDVI Sentinel-2 time series described above; for the vicinity of point **B**, the chip is a rectangle of 16 rows by 19 columns, whereas for point **C**, the corresponding chip is 7×8. Below are details of this analysis.

2.5.1 Imputation by climatology curve Due to the significant loss of information in the analyzed time series, see Figure 4 below, a fully data-dependent gap-filling approach was considered for data in these chips; by doing so, we intended to *let the data speak* and allow for a gap-filling process that borrows strength from the data itself. The method utilized here consisted of taking a quantile of the so-called *climatology curve* as an estimate/prediction/imputation of a missing value in a time series (taken at the pixel level).

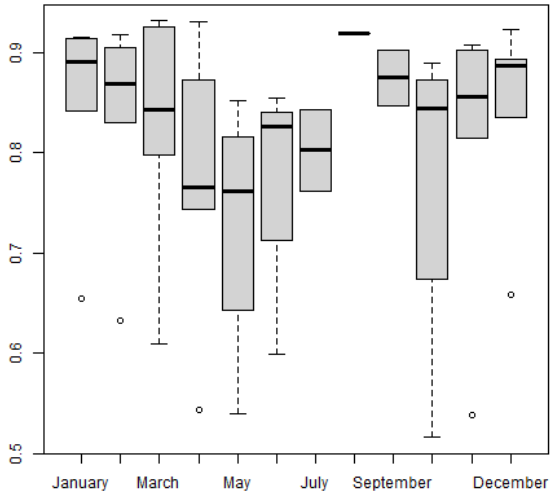

Figure 2. Climatology curve for a pixel nearby **C** in Figure 1.

A climatology curve can be construed as a time-dependent sequence of boxplots. Within a climatology curve, each timepoint represents a data acquisition date; for instance, in this study monthly composites were considered, so the acquisition dates are months. At any acquisition date, the corresponding boxplot is an approximation of the distribution of frequencies of those NDVI values recorded at the same acquisition date across the years/periods of the time series. Thus, it is expected that general seasonal or phenological characteristics within the time series are captured by the climatology curve.

Being based on boxplots (approximation to a probability distribution), in essence, we could use any quantile of the NDVI's distribution and use it to fill those missing values occurring at a given acquisition date. In this study, and aiming for comparison of further results, 25%, 50% (also known as the median, in Figure 3 this quantile is marked at the horizontal black solid line) and the 75% quantiles were considered to fill gaps in the time series. We stress that this methods were only applied to chips **B** and **C** of Figure 1.

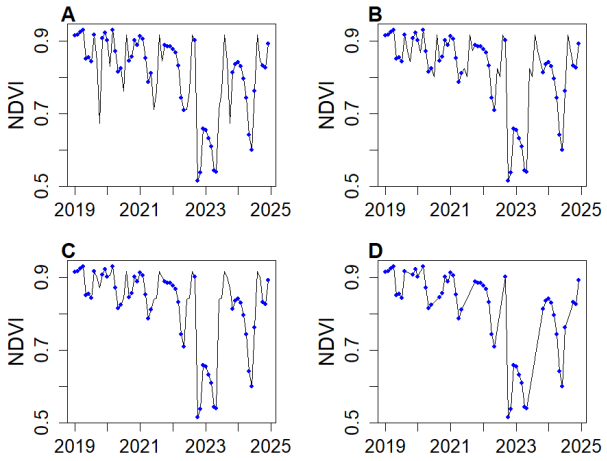

Figure 3. Imputation of missing values using different quantiles of the climatology curve: **A** 25%, **B** 50%, **C** 75%. **D** linear interpolation. Blue points show the original data in the time series.

2.5.2 Trend classification Following (De Jong et al., 2013), the R package bfast was applied to the NDVI time series in order to determine the existence of a change-point in its trend, cf. (Verbesselt et al., 2010). A subsequent application of the function bfast01, allows us to classify these trends in one of the following categories. Let τ denote a change-point, then, we have:

1. **Greening**: increasing linear global trend.
2. **Browning**: decreasing linear global trend.
3. **Sustained greening**: increasing linear local trend before and after τ; at τ the trend is upwards.
4. **Sustained browning**: decreasing linear local trend before and after τ; at τ the trend is downwards.
5. **Delayed greening**: increasing linear local trend before and after τ; at τ the trend is downwards.
6. **Delayed browning**: decreasing linear local trend before and after τ; at τ the trend is upwards.
7. **Greening to browning**: increasing local trend before τ with a decreasing local trend after τ.
8. **Browning to greening**: decreasing local trend before τ with an increasing local trend after τ.

Recently, (Tecuapetla-Gómez et al., 2025) proposed that pixels classified as Browning, Sustained Browning, or Greening to Browning should be considered candidates for potential restoration. Conversely, pixels falling into the categories Delayed Greening or Browning to Greening may indicate areas undergoing natural regeneration. These classification schemes offer a valuable framework for the continuous monitoring of ecosystem condition and resilience

This contribution has been peer-reviewed. The double-blind peer-review was conducted on the basis of the full paper.
https://doi.org/10.5194/isprs-annals-X-3-W3-2025-109-2026 | © Author(s) 2026. CC BY 4.0 License.

2.6 Validation

The results of the trend analyses (Z statistic and trend classification) were visually reviewed in the geographic information system QGIS, and several sites showing either negative or positive trends were verified using field data collected between 2023 and 2024. High-resolution imagery available through Google Earth was also used to support this verification.

3. Results and Discussion

The percentage of available data ranged from 60% to 82% throughout the AOI. The northern zone exhibited the highest data availability, while the lowest values were found in the southern zone. In the central part of Marismas Nacionales, availability remained between 70% and 75%, with clusters of missing data due to cloud cover during certain months. Regarding the number of consecutive missing data points (max-gap length), values ranged from 2 to 6, with higher values in the south and lower values in the north. The months with the least data availability corresponded to the rainy season, between July and September (Figure 4). From this figure, well-defined spatial patterns in data absence are observed; these patterns may be related to the visitation schedules of Sentinel satellites. For the analysis across the entire area, gaps were filled using linear interpolation —a computationally efficient and robust solution (Colditz et al., 2008).

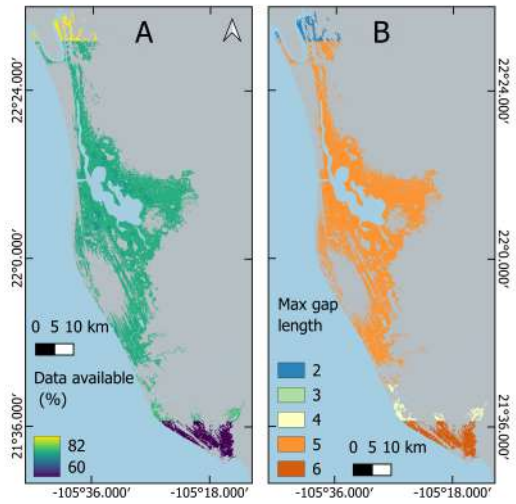

Figure 4. **A** Percentage of available data. **B** Max gap length.

Figure 6 displays the spatial distribution of Z-statistic values estimated from the pixel-level NDVI time series. In general, negative values were observed in the central region of Marismas Nacionales (highlighted in red), corresponding to mangrove areas impacted by Hurricane Roslyn in 2022. The trend classification described above was performed on chips located in this area. In both chips the only significant change-point was found in 2022. In the first chip (**B** in Figure 1) there is a marked presence of the Delayed greening class, followed by the Browning to greening class; a marginal presence of Greening to browning is also acknowledge, see Figure 5. For the second chip (**C** in Figure 1) there is only presence of the Browning to greening class. These results are qualitatively similar independently of the employed gap-filling method -imputation via climatology curve (with any of the three quantiles considered here) and linear interpolation.

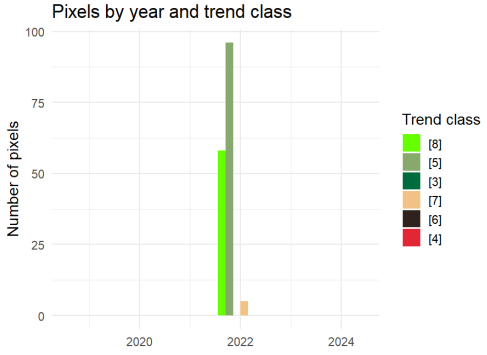

Figure 5. Trend classification during 2019-2024 for time series located in a vicinity of **B** in Figure 1. Results are derived using median-based imputation along the climatology curve.

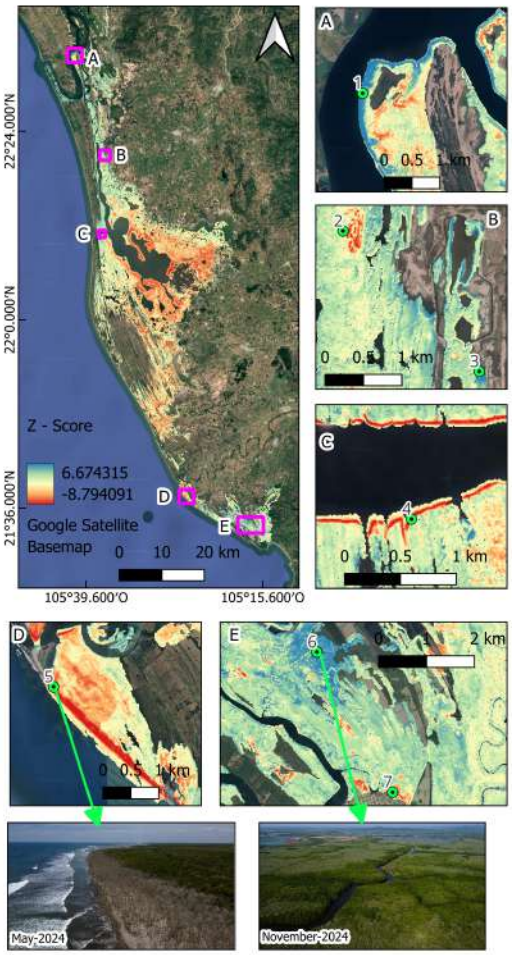

Figure 6. Mann-Kendall's Z-statistic spatial distribution.

These defoliation effects were documented in greater detail by (Velázquez-Salazar et al., 2025), and the affected areas identified in that study coincide with those detected here. Although (Velázquez-Salazar et al., 2025) employed a different methodology—based on interannual anomaly detection using the CMRI index and a linear trend analysis during the post-hurricane period —a correspondence was observed between the hurricane-affected zones and the lowest Z-statistic values, as well as significant negative trends.

This contribution has been peer-reviewed. The double-blind peer-review was conducted on the basis of the full paper.
https://doi.org/10.5194/isprs-annals-X-3-W3-2025-109-2026 | © Author(s) 2026. CC BY 4.0 License.

In the northern zone of the AOI (Figure 6A), areas with high positive Z-statistic values were identified, corresponding to mangrove surfaces impacted by Hurricane Willa in 2018 that have shown a recovery in greenness during the study period. These values are corroborated by the time series (point id-1) in Figure 7 below, which displays a gradual increase in greenness throughout the entire time series. This recovery aligns with findings reported by (Vizcaya-Martínez et al., 2022).

Figure 6B presents two cases (point id-2 and id-3) that illustrate both loss and gain in vegetation greenness. Point 2 represents a decline in greenness within the mangrove coverage, while point 3 indicates an increase in greenness due to inland colonization by the species *Avicennia germinans*. In the case of point 2, no apparent cause for the disturbance could be determined, suggesting the need for further investigation. In contrast, high-resolution imagery revealed hydrological restoration works near point 3, which may be fostering favorable conditions for the species to thrive. This colonization process has also been documented in other regions of the world (Godoy and Lacerda, 2015), where rising mean sea levels have expanded flood-prone areas, creating suitable conditions for the natural establishment of mangroves—provided no physical barriers are present. Although such processes are typically assessed by comparing mangrove coverage with historical data spanning past decades, the present study offers only short-term evidence of this effect, as it highlights increasing greenness in inland zones indicative of emerging vegetation.

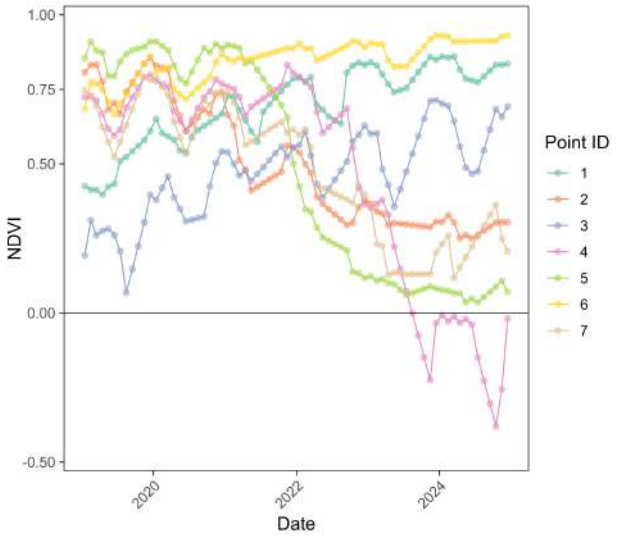

Figure 7. Time series of points referred to in Figure 6 are highlighted here.

Above Figure 6C presents case point id-4, which illustrates mangrove loss due to coastal erosion along the Cuautla Canal. The canal was opened in 1976 and has since expanded steadily, disrupting the hydrology of the entire lagoon system (Valderrama-Landeros et al., 2020). This case exemplifies how the canal's continued growth has resulted in at least 40 meters of erosion on each side, directly affecting mangrove coverage. As shown in Figure 7, NDVI values for point id-4 in recent dates (at least since 2023) fall below zero, indicating the presence of open water. (Valderrama-Landeros et al., 2020) estimated a loss of 805 hectares of beach deposits between 1970 and 2019 along the Cuautla Canal, based on coverage derived from aerial photographs and satellite imagery (Landsat, Spot-5, and Sentinel-2). Although their study concludes in 2019, the same erosive process persists into the period analyzed in the present study, suggesting that the system has yet to stabilize and may continue to degrade in the coming years.

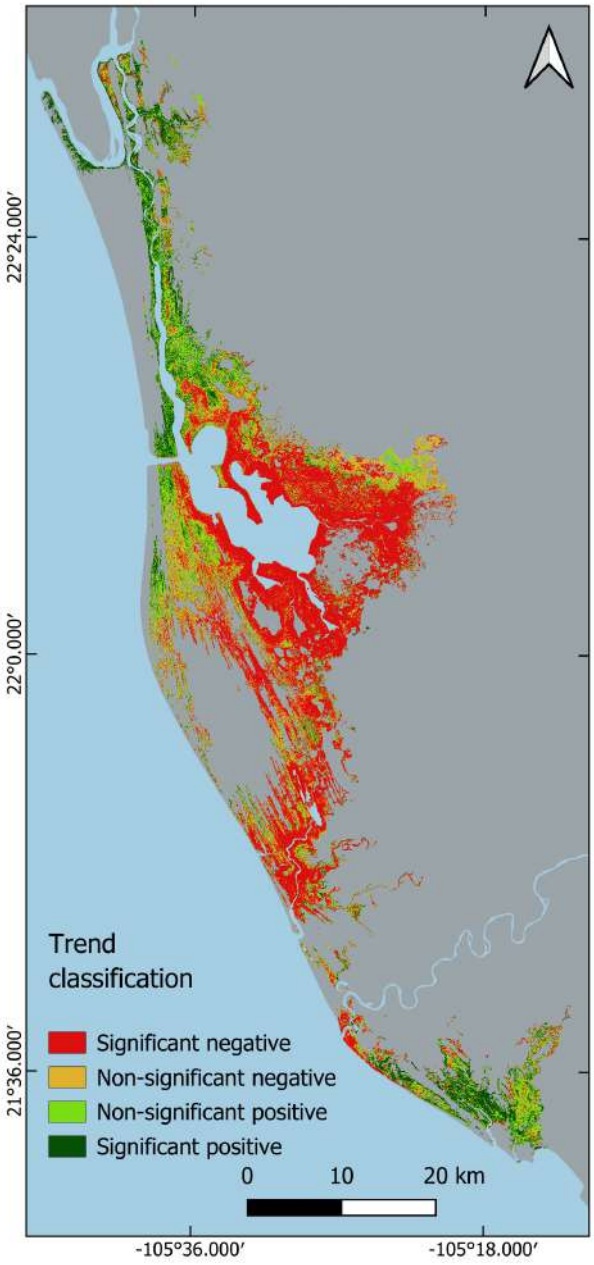

Figure 8. Trend classification based on Mann-Kendall test statistical significance; a p-value test below 0.05 defines a significant pixel in this map.

This process of mangrove loss due to coastal erosion was also observed in Figure 6D, where point id-5 represents an area of declining greenness. (Valderrama-Landeros et al., 2020) describe this coastal erosion as resulting from changes in sediment dynamics caused by upstream damming. Figure 6 (bottom row, left) shows a photograph taken in May 2024, where the dead mangrove front at point id-5 is clearly visible. Combining Figure 6 (bottom row, right) with Figure 7 point-id 6, it can be seen that starting in November 2021, greenness rises and NDVI values remain high through December 2024.

The area with the highest Z-statistic values was identified in

This contribution has been peer-reviewed. The double-blind peer-review was conducted on the basis of the full paper.
https://doi.org/10.5194/isprs-annals-X-3-W3-2025-109-2026

the southern part of the AOI (point id-6, Figure 6E). This zone was not impacted by hurricanes during the study period and may be influenced by nutrient inputs from nearby shrimp farms. Meanwhile, 2.5 km to the south, in the vicinity of the port of San Blas (Figure 6E, point id-7), areas of loss were identified due to land-use change. For both cases, Figure 7 shows the NDVI values over time during the study period, with point id-6 standing out for having the highest values recorded among the examples.

Across the 80,959 hectares encompassed by the study area, 47.08% exhibited a significant negative trend, 20.19% a non-significant negative trend, 18.07% a non-significant positive trend, and 14.66% a significant positive trend (Figure 8). These data reveal the dynamic nature of the mangrove ecosystem in response to various change drivers, its resilience to hydrometeorological disturbances, its sensitivity to coastal erosion, and its capacity to colonize new areas at the expense of marshlands.

4. Conclusions

The methodologies applied for monitoring the mangrove ecosystem—based on a six-year NDVI time series (2019–2024) in Marismas Nacionales—enabled the identification of diverse vegetation change processes specific to this region. These include disturbance and recovery dynamics triggered by hydrometeorological events, inland colonization, coastal erosion losses, land-use change, and restoration interventions. Collectively, these patterns underscore the ecosystem's dynamic behavior, its resilience, and its vulnerability to climate change. This continuous monitoring framework holds promise for national-scale implementation, offering a robust tool to detect ecological processes across diverse regions. The resulting data could serve as a foundational input for public policies aimed at mangrove conservation and restoration.

Acknowledgment

The World Wildlife Fund (WWF), with support from The Bezos Earth Fund, provided financial support through agreement MX13531 "Strengthening the Mexico's Mangrove Monitoring System (SMMM)", granted to CONABIO. Also, the "Comisión Nacional de Áreas Naturales Protegidas (CONANP)" authorized the following permits for scientific endeavors conducted within the confines of the natural protected area Marismas Nacionales: DROPC/RBMNN/055/2023, DROPC/RBMNN/069/2023, DROPC/RBMNN/153/2023, DROPC/RBMNN/173/2023, and DROPC/RBMNN/071/2024. The "Instituto Nacional de Estadística y Geografía (INEGI)" and the "Secretaría de la Defensa Nacional (SEDENA)" provided the following permits to operate the Matrice 300-UAV drone: LA0032023, LA0222023, LA0952023, LA1002023, LA0122024, and LA0212024.

References

Abu Bakar, N. A., Wan Mohd Jaafar, W. S., Abdul Maulud, K. N., Muhmad Kamarulzaman, A. M., Saad, S. N. M., Mohan, M., 2024. Monitoring mangrove-based blue carbon ecosystems using UAVs: a review. *Geocarto International*, 39(1), 2405123.

Colditz, R. R., Conrad, C., Wehrmann, T., Schmidt, M., Dech, S., 2008. TiSeG: A flexible software tool for time-series generation of MODIS data utilizing the quality assessment science data set. *IEEE transactions on geoscience and remote sensing*, 46(10), 3296–3308.

De Jong, R., Verbesselt, J., Zeileis, A., Schaepman, M. E., 2013. Shifts in global vegetation activity trends. *Remote Sensing*, 5(3), 1117–1133.

de la Lanza Espino, G., Rodríguez, I. P., Czitrom, S. P., 2010. Water quality of a port in NW Mexico and its rehabilitation with swell energy. *Marine Pollution Bulletin*, 60(1), 123–130.

Ferreira, A. C., De Lacerda, L. D., Rodrigues, J. V. M., Bezerra, L. E. A., 2023. New contributions to mangrove rehabilitation/restoration protocols and practices. *Wetlands Ecology and Management*, 31(1), 89–114.

Floriano, B. R., Hanson, B., Bewley, T., Ishihara, J. Y., Ferreira, H. C., 2025. A novel policy for coordinating a hurricane monitoring system using a swarm of buoyancy-controlled balloons trading off communication and coverage. *Engineering Applications of Artificial Intelligence*, 139, 109495.

Godoy, M. D., Lacerda, L. D. d., 2015. Mangroves response to climate change: a review of recent findings on mangrove extension and distribution. *Anais da Academia Brasileira de Ciências*, 87(2), 651–667.

Hao, Q., Song, Z., Zhang, X., He, D., Guo, L., van Zwieten, L., Yu, C., Wang, Y., Wang, W., Fang, Y. et al., 2024. Organic blue carbon sequestration in vegetated coastal wetlands: Processes and influencing factors. *Earth-Science Reviews*, 255, 104853.

Islam, A. M., Assal, T. J., 2023. Rapid, landscape-scale assessment of cyclonic impacts on mangrove forests using MODIS imagery. *Coasts*, 3(3), 280–293.

R Core Team, 2023. R: A Language and Environment for Statistical Computing. R Foundation for Statistical Computing, Vienna, Austria.

Tecuapetla-Gómez, I., López-Saldaña, G., Cruz-López, M. I., Ressl, R., 2021. TATSSI: A free and open-source platform for analyzing earth observation products with quality data assessment. *ISPRS International Journal of Geo-Information*, 10(4), 267.

Tecuapetla-Gómez, I., Velázquez-Salazar, S., Gómez-Juárez, E., 2025. First steps for detecting potential forest restoration zones in Southeastern Mexico. *IGARSS 2025-2025 IEEE International Geoscience and Remote Sensing Symposium*, IEEE, To appear.

Valderrama, L., Troche, C., Rodriguez, M. T., Marquez, D., Vázquez, B., Velázquez, S., Vázquez, A., Cruz, M. I., Ressl, R., 2014. Evaluation of mangrove cover changes in Mexico during the 1970–2005 period. *Wetlands*, 34(4), 747–758.

Valderrama-Landeros, L., Blanco y Correa, M., Flores-Verdugo, F., Álvarez-Sánchez, L. F., Flores-de Santiago, F., 2020. Spatiotemporal shoreline dynamics of Marismas Nacionales, Pacific coast of Mexico, based on a remote sensing and GIS mapping approach. *Environmental Monitoring and Assessment*, 192(2), 123.

Valderrama-Landeros, L., Camacho-Cervantes, M., Velázquez-Salazar, S., Villeda-Chávez, E., Flores-Verdugo, F., Flores-de Santiago, F., 2025. Detection of an invasive plant (Cissus verticillata) in the largest mangrove system on the eastern Pacific coast—a remote sensing approach. *Wetlands Ecology and Management*, 33(1), 13.

Velázquez-Salazar, S., Rodríguez-Zúñiga, M., Alcántara-Maya, J., Villeda-Chávez, E., Valderrama-Landeros, L., Troche-Souza, C., Vázquez-Balderas, B., Pérez-Espinosa, I., Cruz-López, M., Ressl, R. et al., 2021. Manglares de México. Actualización y análisis de los datos 2020. *Comisión Nacional para el Conocimiento y Uso de la Biodiversidad. CDMX México*.

Velázquez-Salazar, S., Valderrama-Landeros, L., Villeda-Chávez, E., Cervantes-Rodríguez, C., Troche-Souza, C., Alcántara-Maya, J., Vázquez-Balderas, B., Rodríguez-Zúñiga, M., Cruz-López, M., Flores-de Santiago, F., 2025. Mangrove Damage and Early-Stage Canopy Recovery Following Hurricane Roslyn in Marismas Nacionales, Mexico. Forests 2025, 16, 1207. https. *doi. org/10.3390/f16081207*.

Verbesselt, J., Hyndman, R., Zeileis, A., Culvenor, D., 2010. Phenological change detection while accounting for abrupt and gradual trends in satellite image time series. *Remote Sensing of Environment*, 114(12), 2970–2980.

Vizcaya-Martínez, D. A., Flores-de Santiago, F., Valderrama-Landeros, L., Serrano, D., Rodríguez-Sobreyra, R., Álvarez-Sánchez, L. F., Flores-Verdugo, F., 2022. Monitoring detailed mangrove hurricane damage and early recovery using multi-source remote sensing data. *Journal of Environmental Management*, 320, 115830.